Supplement of Clim. Past, 12, 299–316, 2016
http://www.clim-past.net/12/299/2016/
doi:10.5194/cp-12-299-2016-supplement
© Author(s) 2016. CC Attribution 3.0 License.

Supplement of

Frequency and intensity of palaeofloods at the interface of Atlantic and Mediterranean climate domains

B. Wilhelm et al.

Correspondence to: B. Wilhelm (bruno.wilhelm@ujf-grenoble.fr)

The copyright of individual parts of the supplement might differ from the CC-BY 3.0 licence.

Chronology: detailed methods for palaeomagnetic investigations

Palaeomagnetic investigations were performed at the CEREGE laboratory (Aix-Marseille University) on cores FOR13P1, FOR13P2 and FOR13P4 using u-channels sub-samples. The natural remanent magnetization (NRM) was progressively demagnetized using alternating fields with 10, 20, 30, 40, 60, 80 and 100 mT steps. In order to distinguish different mineralogical and grain-size fractions within the magnetic components, two types of laboratory remanent magnetizations were conducted: Isothermal Remanent Magnetization (IRM) and Anhysteretic Remanent Magnetization (ARM). ARM was produced in-line along the u-channel axis, using a 100 mT alternating field with a superimposed 0.05 mT steady field. IRM was obtained by passing the u-channels through two different Halbach cylinders that develop fields of 1 and 0.3 T, respectively (Rochette et al., 2001). For ARM and IRM1T, demagnetization was done following steps of 10, 20, 30, 40, 60, 80 and 100 mT. The magnetizations have been measured before alternating-field treatment and after each step using the 3-axis 2-G enterprise cryogenic magnetometer located in a shielded room. Additionally, anisotropy of magnetic susceptibility has been measured using AGICO MFK1-FA Kappabridge (spinning specimen method) to control the preservation of the sedimentary fabric. The susceptibility ellipsoid is defined by three eigenvectors (Kmax, Kint and Kmin). The magnetic fabric is usually comparable to the sediment fabric with inclination of the Kmin close to the vertical (Borradaile, 1988; Rochette et al., 1992; Tarling and Hrouda, 1993).

	Flood date	Affected rivers	Spatial extent of the flood	Victim	Damage	Disruptions	Details on the hydro-meteorological causes
>	3 September 2012	Guil	Ristolas and villages downstream	N	Y	Y	Easterlies winds with heavy rainfalls in the upper part of catchment
	28 May 2008	Guil	Ristolas and villages downstream	Y	Y	Y	Heavy rainfall event
	13 June 2002	Torrents of Segure and other	Ristolas	N	N	N	Heavy rainfalls mainly in the upper part of the catchment
>	15 July 2002	Guil	Ristolas and villages downstream	N	Y	Y	Easterlies winds with heavy rainfalls in the upper part of the catchment
>	15 October 2000	Guil and other	Ristolas and villages downstream	N	Y	N	5 days of heavy rainfalls with increased rainfall depths the last 2 days
	13 June 2000	Guil and Torrent of Segure	Ristolas and villages downstream	N	Y	Y	Heavy rainfalls mainly in the upper part of the catchment
>	July 1992	Torrent of Bouchouse	Ristolas	N	Y	Y	Violent thunderstorms
	11 June 1978	Guil	Ristolas and villages downstream	N	Y	U	
	5 May 1973	Guil	Ristolas and villages downstream	N	Y	U	
>	1 November 1963	Undefined	Ristolas	N	Y	U	
	21 May 1959	Guil	Ristolas and villages downstream	N	Y	Y	
>	Summer 1959	Guil	Ristolas and villages downstream	N	U	Y	
	13 June 1957	Guil and Torrent of Segure	Ristolas and villages downstream	N	Y	Y	Heavy rainfalls, thunderstorm, snowmelt
>	October 1953	Torrent of Jalinette	Ristolas	N	Y	Y	Heavy rainfall event
>	29 Sept. 1953	Guil	Ristolas and villages downstream	N	Y	Y	Heavy rainfall event during 3 days
>	1 July 1953	Torrent of Jalinette	Ristolas	N	Y	Y	
	8 June 1953	Guil	Ristolas and villages downstream	N	Y	Y	Violent thunderstorms and snowmelt
	14 May 1948	Guil	Ristolas and villages downstream	Y	Y	Y	Rainfall depth of 244 mm in 3 days, with snowmelt
>	4 August 1938	Torrent of Segure	Ristolas	N	Y	Y	Violent thunderstorms
	1932	Torrent of Maloqueste	Ristolas	N	Y	U	
>	9 July 1932	Guil	Ristolas and villages downstream	N	Y	Y	
>	1 September 1920	Guil	Ristolas and villages downstream	N	Y	Y	
	29 May 1856	Guil	Ristolas and villages downstream	N	U	U	Heavy rainfalls over a long period before the flood event
>	6 August 1852	Guil	Ristolas and villages downstream	N	Y	Y	Heavy rainfall events
>	15 October 1839	Guil	Ristolas and villages downstream	N	Y	U	Heavy rainfall events
>	13 Sept. 1810	Guil and Torrent of Segure	Ristolas and villages downstream	N	Y	Y	Heavy rainfall events during 8 days
>	13 October 1810	Guil	Ristolas and villages downstream	N	Y	Y	
>	10 October 1791	Guil and Torrent of Chapelle	Ristolas and villages downstream	N	Y	Y	
>	9 October 1790	Guil	Ristolas and villages downstream	N	Y	Y	
	1789	Guil	Ristolas and villages downstream	N	Y	Y	
>	07 Sept. 1788	Guil	Ristolas and villages downstream	N	Y	Y	
>	7 September 1787	Guil	Ristolas and villages downstream	N	Y	U	
>	4 October 1751	Guil	Ristolas and villages downstream	N	U	U	Heavy rainfall events

Table S1. List of historical flood events which runs through the village of Ristolas, located 8 km downstream from Lake Foréant (from the free-access database of the ONF-RTM, http://rtm-onf.ifn.fr/). The arrows in the first row highlight the floods that occurred in summer and fall, i.e. that may be recorded in the lake sediments because this period corresponds to the ice-free season of Lake Foréant. N means No, Y means Yes and U, Uncertain.

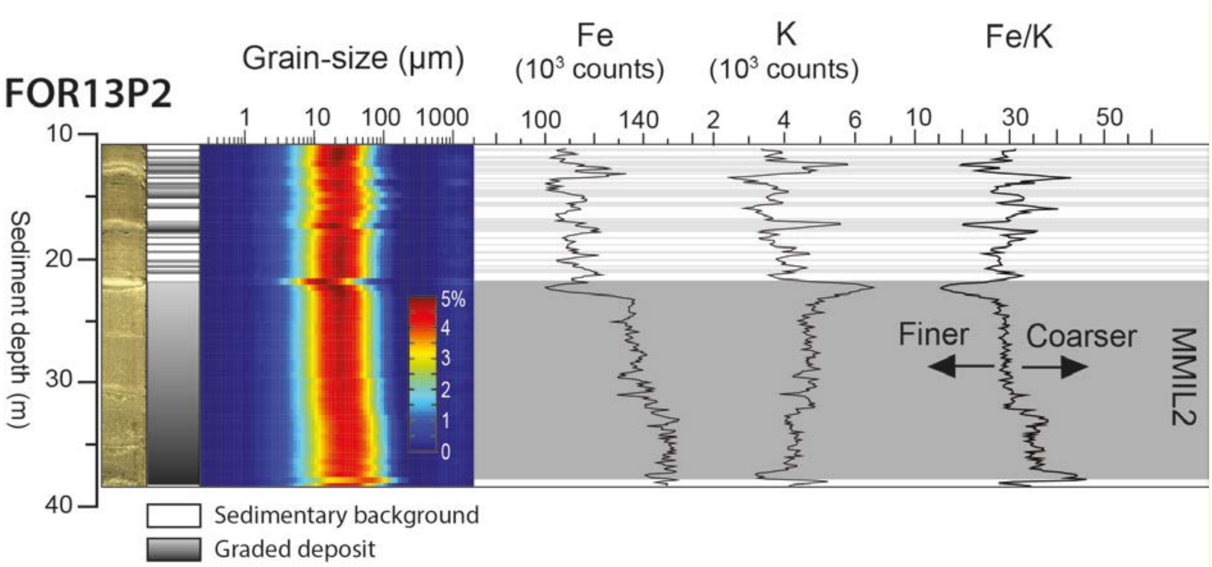

Fig. S1. Zoom of the grain-size variability and associated geochemical proxy for core FOR13P2. Refer to Figure 2 and to the main text for details.

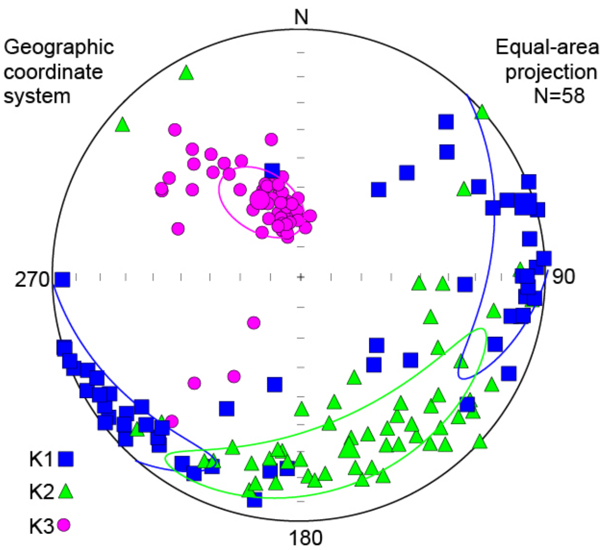

Fig. S2. Results of Anisotropy of Magnetic Susceptibility for core FOR13P4: stereo plot of the main axes direction. Notice that the K3 is well grouped and close to the vertical except some points associated with MMITs.

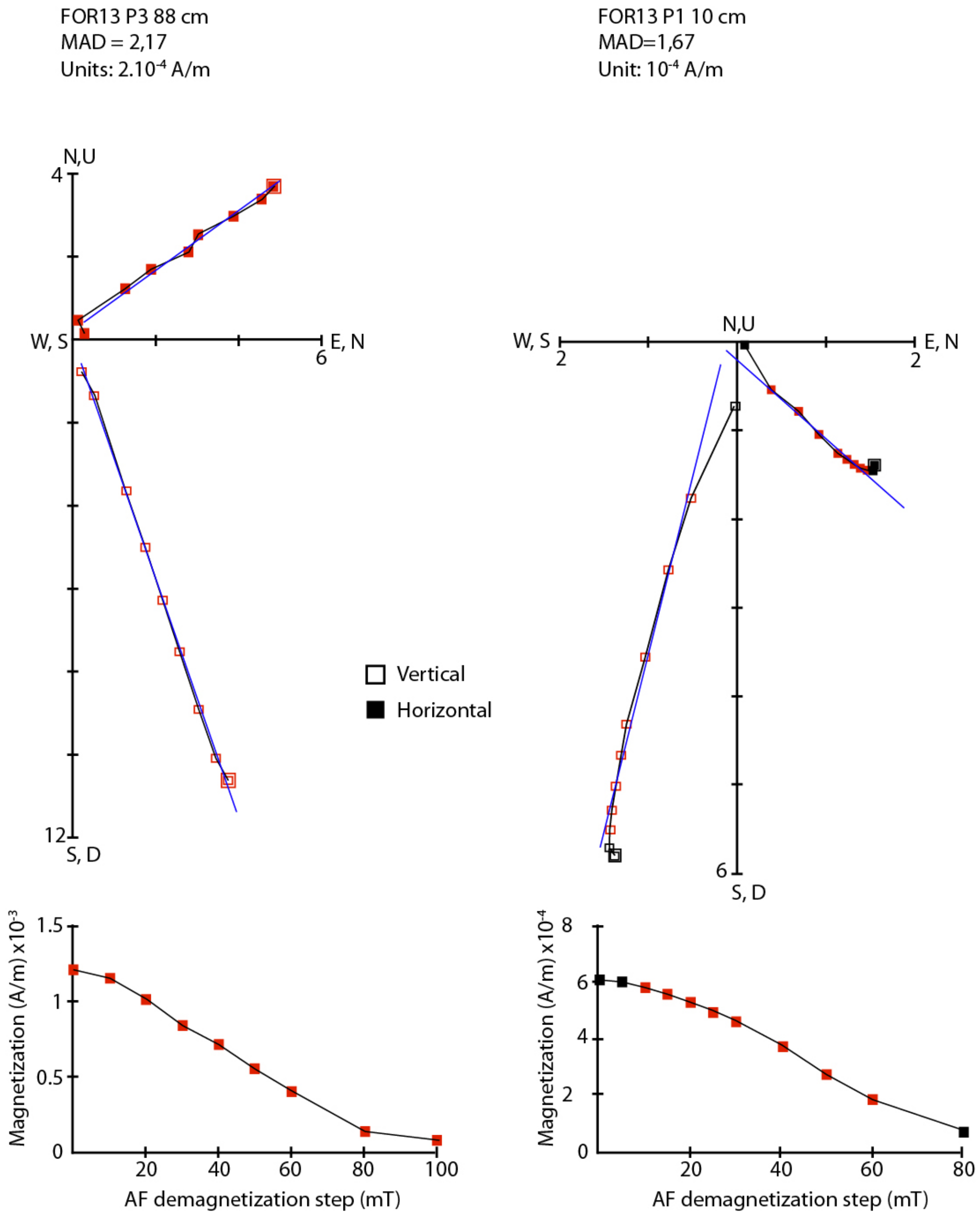

Fig. S3. Example of stepwise alternating field demagnetization of NRM (orthogonal vector projections and intensity curves) for representative samples. Solid (open) symbols are horizontal (vertical) plane projections.

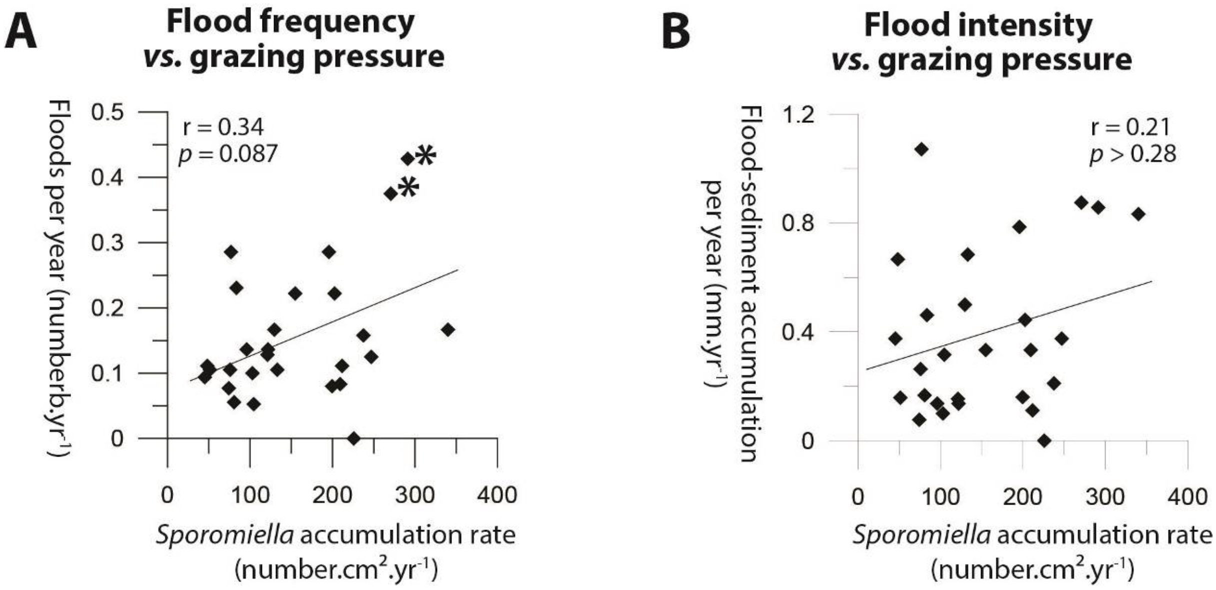

Fig. S4. Representation and correlation coefficients (r) of relations between (A) *Sporormiella* accumulation rates (number.cm².yr^{-1}) and floods frequency (nb.yr^{-1}), and between (B) *Sporormiella* accumulation rates (number. cm² yr-1) and flood-sediment accumulation (mm.$years^{-1}$). The stars identified two samples, dated from 1734 to 1760 AD, with both high grazing pressure and high flood frequency. Levels of significance (*p* values) were determined using a Spearman-test.

References

Rochette, P., Jackson, M., Aubourg, C.: Rock magnetism and the interpretation of anisotropy of magnetic susceptibility, Reviews of Geophysics 30 (3), 209–226, 1992.

Rochette, P., Vadeboin, F., Clochard, L.: Rock magnetic applications of Halbach cylinders, Physics of the Earth and Planetary Interiors 126, 109–117, 2001.

Borradaile, G.: Magnetic susceptibility, petrofabrics and strain, Tectonophysics, 156, 1–20, 1988.

Tarling, D.H., Hrouda, F.: The Magnetic Anisotropy of Rocks, Chapman & Hall, London (218 pp.), 1993.